Dust attenuation in Ultra Dusty Star-Forming galaxies up to z $\sim$ 4

Mahmoud Hamed[1] and Katarzyna Małek[1,2]

1. National Centre for Nuclear Research, ul. Pasteura 7, 02-093 Warszawa, Poland
2. Aix Marseille Univ. CNRS, CNES, LAM, Marseille, France

Despite its low contribution to the total mass of the interstellar medium (ISM), dust plays a crucial role in the evolution of galaxies. Moreover, the dust properties have crucial impact on the shape of the galaxy spectral energy distribution. The affluence of infrared and radio detections of millions of galaxies in the COSMOS field, provided by powerful instruments such as *Herschel* and ALMA, has allowed to study the cold dust in galaxies over a wide range of redshift. A key element in reproducing the total spectral energy distribution of galaxies, is assuming a dust attenuation law which accounts for the behavior and the imprints of dust in the ISM. However, different studies have shown that widely used in the literature single law cannot fully model dust in a large sample of galaxies. This non-universality of attenuation laws should be considered in order to accurately account for dust, and therefore in deriving the physical properties of galaxies. In this work, we study different attenuation laws in a statistical sample of ALMA-detected galaxies in the COSMOS field. We probe the resulting variation of key physical properties of these galaxies such as the stellar mass and spatial extent of the dust continuum and the implication that it might have on the attenuation curve. We find that a bouquet of attenuation curves must be used in order to reproduce the UV spectrum. Although these curves are not redshift dependent, they are correlated to the relative spatial distribution to the stellar population of heavily dust-obscured galaxies.

1 Introduction

The young Universe did not only undergo more star formation rates (SFRs), but a non-negligent fraction of this SFR was obscured by interstellar dust (e.g., Madau & Dickinson, 2014; Gruppioni et al., 2020). During this time, the heavily attenuated in the ultraviolet (UV) dusty star-forming galaxies (DSFGs, e.g. Casey et al., 2014; Béthermin et al., 2015; Casey et al., 2017; Donevski et al., 2020) have contributed massively to the cosmic SFR, making them instrumental to the comprehension of galaxy evolution.

Interstellar dust is tremendously efficient in absorbing short wavelength photons, originating from massive young stars, making an important fraction of star-forming clouds of galaxies inaccessible. This attenuated light can be successfully reproduced by assuming a dust attenuation law (e.g., Burgarella et al., 2005; Buat et al., 2012, 2014; Lo Faro et al., 2017; Salim et al., 2018; Salim & Narayanan, 2020).However, a single attenuation law cannot reproduce dust attenuation in the interstellar medium (ISM) of a large and diverse sample of galaxies (e.g., Buat et al., 2018; Małek et al., 2018; Salim & Narayanan, 2020). When modeling dust attenuation, different approaches appear to work in reproducing spectral energy distributions (SEDs) of

galaxies. Calzetti et al. (2000) assumed a single component dust-to-stars distribution by measuring the extinction in local starburst galaxies. The steep attenuation curve of Calzetti et al. (2000) succeeds in modeling dust reddening even at high-redshift metal-poor galaxies with bright cold dust component. The double component dust attenuation of Charlot & Fall (2000) assumes a more complex, patchy distribution. With this approach, newly formed stars are placed in the cold molecular clouds, and experience double attenuation by dust of the molecular clouds and the ISM. Older stars are attenuated by the dust grains of the ISM alone. These attenuation laws, together with their different recipes, are often used in the literature when modeling the SED of galaxies. However, dust attenuation curves are not universal, and they significantly alter the physical properties of galaxies such as their stellar masses (Małek et al., 2018; Buat et al., 2019). Therefore, it is crucial for the global understanding of galaxy evolution to study the behavior of dust attenuation and understand the factors that can affect the shape of attenuating short wavelength spectra.

2 Data

The sample of galaxies used for this work comes from the COSMOS field (Scoville et al., 2007; Ilbert et al., 2013; Laigle et al., 2016). The choice of COSMOS field is motivated by the abundance of multiwavelength data spanning accross a wide range of redshifts, as well as the significant number of ALMA detections that this field experienced.

2.1 Photometric data

The photometric data of our sample comes from the *Herschel* Extragalactic Legacy Project (HELP) panchromatic catalog (Shirley et al., 2019, 2021). To achieve the HELP catalog, *Herschel* fluxes were extracted using XID+ (Hurley et al., 2017), a probabilistic deblender of SPIRE maps, that takes into account the positions of sources detected with *Spitzer* at 24 μm detections which are more resolved. This technique increases the accuracy of FIR flux extraction along with further estimation of photometric redshift (Duncan et al., 2018).

To build a statistically important sample and to well constrain its physical properties, we selected galaxies that have at least 10 detections in the UV to near-IR (NIR) (0.3 - 8 μm) range with S:N $>$ 5. We also required at least 6 detections in the NIR-FIR bands (8 - 1000 μm) out of which at least 3 detections having a S:N $>$ 3. Above-mentioned criteria allow to select galaxies perfectly suited for detailed modeling but also the brightest, and the most massive galaxies, which can imply selection bias. For sources that have detections in similar bandpass filters, we use the fluxes acquired from the deeper survey.

2.2 ALMA data

The ALMA fluxes and continuum maps used in this paper are the result of the A^{3}COSMOS automated ALMA data mining in the COSMOS field (Liu et al., 2019). A^{3}COSMOS gathers into one catalog more than 1 000 identified sources from more than a decade worth of different projects with different scientific aims. We perform a positional cross-match with the HELP catalog with a conservative 1" search radius.

2.3 Final sample

The above described selection yields in the final sample of 316 galaxies, covering a redshift range of $0.2 < z < 4.2$. More than 30% of the sample, 96 galaxies, have spectroscopic redshifts. We used the photometric redshifts provided by the HELP catalog for the remaining 222 galaxies. Table 1 shows the photometric bands used for our data and the associated S:N for our final sample.

Tab. 1: Summary of available photometric data in each band with its centered wavelength, the median of S:N and the number of detections in our sample.

Telescope/ Instrument	Band	λ [μm]	Median S:N	Nº of detections
CFHT/ MegaCam	u	0.38	11.12	251
	g	0.49	22.39	265
	r	0.62	25.55	280
	i	0.75	26.48	283
	z	0.89	16.58	276
Subaru/ Suprime-Cam	B	0.44	12.97	272
	V	0.54	11.78	303
	Y	0.98	8.02	237
VISTA	Y	1.02	5.73	8
	J	1.25	33.68	310
	H	1.65	43.69	311
	Ks	2.15	65.39	311
Spitzer/ IRAC	ch1	3.56	136.93	316
	ch2	4.50	146.94	316
	ch3	5.74	9.62	316
	ch4	7.93	5.95	312
Spitzer/MIPS	MIPS1	23.84	40.17	316
Herschel/ PACS	100 μm	102.62	2.34	316
	160 μm	167.14	1.33	316
Herschel/ SPIRE	250 μm	251.50	12.44	316
	350 μm	352.83	7.47	316
	500 μm	511.60	3.08	316
ALMA	7	947	8.73	200
	6	1255	8.76	112
	4	2100	5.01	2
	3	3076	4.67	2

3 Methods

3.1 Spectral energy distribution fitting

To derive the physical properties of our well-constrained multiwavelength sample, we use the Code Investigating GALaxy Emission `CIGALE`[1], an energy balance technique

[1] `https://cigale.lam.fr/`

of the SED fitting (Noll et al., 2009; Boquien et al., 2019). This technique of SED fitting takes into account the energetic balance between the rest-frame UV part of the total galaxy emission, and its rest-frame IR emission. The mediator in this energy balance is the dust. `CIGALE` works in the broad band photometry regime. Every wavelength domain of the SED total emission is the final product of complex physical processes that will produce photons at a specific frequency. In the following subsections we describe the main SED components that we considered.

3.1.1 Star formation history

Star formation histories (SFH) are sensitive to many complex factors including galaxy interaction, merging, gas accumulation and its depletion (e.g. Elbaz et al., 2011; Ciesla et al., 2018; Schreiber et al., 2018). The SFHs have a significant effect on fitting the UV part of the SED, and consequent affecting the derived physical parameters such as the stellar masses and the SFRs. Ciesla et al. (2017) showed that simple SFH models (such as a delayed model) are not enough to reproduce a precise fit of the UV data, especially for galaxies that are undergoing a starburst or quenching activity.

To model the SEDs of our IR-bright sample, we use a delayed SFH with a recent exponential burst (e.g. Małek et al., 2018; Buat et al., 2018; Donevski et al., 2020). This recent burst is motivated by the ALMA detection (Hamed et al., 2021), and in such scenario, a galaxy will build the majority of its stellar population in its earlier evolutionary phase, then the star formation activity slowly decreases over time. This is followed by a recent burst of SFR which mimics presence of young stellar population in the galaxy.

3.1.2 Dust absorption and emission

The dust content of our sample of DSFGs is presumed to be the most affecting component of the shapes of the derived SEDs. This makes the modeling of dust attenuation an indispensable priority in order to extract accurate physical properties. To address the dust problem, we use two distinct approaches of emulating attenuation laws for the SED fitting: the approach of Calzetti et al. (2000, hereafter C00) and that of Charlot & Fall (2000, hereafter CF00). While these two attenuation approaches are relatively simple, they differ on how to attenuate a given stellar population. The attenuation curve of C00 was tuned to fit a sample of starbursts in the local Universe, which represent high redshift UV-bright galaxies. This curve attenuates a stellar population with a simple power-law characterized by a power-law slope. Despite its simplicity, this attenuation curve, with its modifications, is widely used in the literature.

Another approach is to consider the dust spatial distribution relative to the stellar population. This is the core of the attenuation curve of CF00. In this approach, dust is considered to attenuate the dense and cooler molecular clouds differently than the diffuse ISM. This configuration is expressed by two independent power-laws. In this work we use the aforementioned laws to model dust attenuation of the galaxies of our sample.

To reproduce the IR emission in our SED models, we use the templates of Draine et al. 2014. These templates take into consideration different sizes of grains of carbon and silicate, hence, allowing different temperatures of dust grains.

3.2 Size measurements

To study the spatial extent of dust emission and that of the stellar populations and the star-forming regions of our sources, we derived the effective radii (R_e) of the dust continuum maps and their short-wavelength counterparts. To achieve this, we used `STATMORPH` code (Rodriguez-Gomez et al., 2019).

4 Results

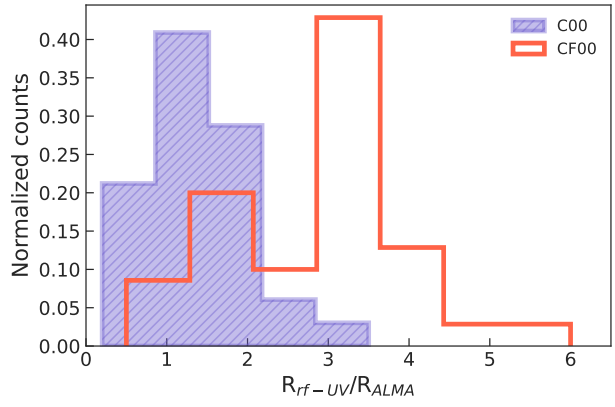

Fig. 1: Rest-frame UV radii of the galaxies of our sample relative to their dust continua, with two different attenuation recipes used: C00 and CF00.

We find that dust attenuation laws whether characterized by their effective attenuating slope or the dust-to-stars geometry, strongly alter derived physical properties of galaxies, mainly their stellar masses. This is indeed expected, since shallower attenuation laws (e.g. Charlot & Fall, 2000; Lo Faro et al., 2017) assume a more attenuated fraction of older stellar population, manifested in efficiently-extinct optical to NIR photons. This is in agreement with Małek et al. (2018) and Hamed et al. (2021). The large differences in produced stellar masses change the loci of galaxies with respect to the main sequence of star-forming galaxies. With quality of SED fits assessment, we assign the best attenuation curve to each galaxy of our sample and we test their physical properties produced by fitting the stellar SEDs, as well as their IR SEDs. We notice that shallower attenuation curves overestimate the stellar masses and the IR luminosities. Based on the quality of the SED fitting with two different attenuation laws, in other words, after checking how good the fit imitates real observation, we have selected the most suitable attenuation law for each galaxy. We have found that CF00 fitted better 79% of the DSFGs of our sample. Moreover, we check the effect of dust distribution relative to the star-forming regions of our sample on the assumed dust attenuation laws as in Buat et al. (2019). We confirm, as shown in Fig. 1, that shallow attenuation curves fitted better galaxies with compact dust distribution relative to the rest frame UV continuum.

Acknowledgements. This work has been supported by the Polish National Science Centre grant No. UMO-2018/30/E/ST9/00082. This work makes use of ALMA data. ALMA is a partnership of ESO, NSF (USA) and NINS (Japan), together with NRC (Canada), MOST and ASIAA (Taiwan), and KASI (Republic of Korea), in cooperation with the Republic of Chile. The Joint ALMA Observatory is operated by ESO, AUI/NRAO and NAOJ. We thank the organizers of the conference.

References

Béthermin, M., et al., *A&A* **573**, A113 (2015)
Boquien, M., et al., *A&A* **622**, A103 (2019)
Buat, V., et al., *A&A* **545**, A141 (2012)
Buat, V., et al., *A&A* **561**, A39 (2014)
Buat, V., et al., *A&A* **619**, A135 (2018)
Buat, V., et al., *A&A* **632**, A79 (2019)
Burgarella, D., Buat, V., Iglesias-Páramo, J., *MNRAS* **360**, 4, 1413 (2005)
Calzetti, D., et al., *ApJ* **533**, 2, 682 (2000)
Casey, C. M., et al., *ApJ* **796**, 2, 95 (2014)
Casey, C. M., et al., *ApJ* **840**, 2, 101 (2017)
Charlot, S., Fall, S. M., *ApJ* **539**, 2, 718 (2000)
Ciesla, L., Elbaz, D., Fensch, J., *A&A* **608**, A41 (2017)
Ciesla, L., et al., *A&A* **615**, A61 (2018)
Donevski, D., et al., *A&A* **644**, A144 (2020)
Draine, B. T., et al., *ApJ* **780**, 2, 172 (2014)
Duncan, K. J., et al., *MNRAS* **473**, 2, 2655 (2018)
Elbaz, D., et al., *A&A* **533**, A119 (2011)
Gruppioni, C., et al., *A&A* **643**, A8 (2020)
Hamed, M., et al., *A&A* **646**, A127 (2021)
Hurley, P. D., et al., *MNRAS* **464**, 1, 885 (2017)
Ilbert, O., et al., *A&A* **556**, A55 (2013)
Laigle, C., et al., *ApJS* **224**, 2, 24 (2016)
Liu, D., et al., *ApJS* **244**, 2, 40 (2019)
Lo Faro, B., et al., *MNRAS* **472**, 2, 1372 (2017)
Madau, P., Dickinson, M., *ARA&A* **52**, 415 (2014)
Małek, K., et al., *A&A* **620**, A50 (2018)
Noll, S., et al., *A&A* **507**, 3, 1793 (2009)
Rodriguez-Gomez, V., et al., *MNRAS* **483**, 3, 4140 (2019)
Salim, S., Boquien, M., Lee, J. C., *ApJ* **859**, 1, 11 (2018)
Salim, S., Narayanan, D., *ARA&A* **58**, 529 (2020)
Schreiber, C., et al., *A&A* **618**, A85 (2018)
Scoville, N., et al., *ApJS* **172**, 1, 1 (2007)
Shirley, R., et al., *MNRAS* **490**, 1, 634 (2019)
Shirley, R., et al., *MNRAS* **507**, 1, 129 (2021)